LabVIEW Implementation of Tuning PID Controller Using Advanced Control Optimization Techniques for Micro-robotics System

Ehab Seif Ghith and Farid Abdel Aziz Tolba
Faculty of Engineering, Ain shams University, Cairo, Egypt
Email: Drehabghith1978@gmail.com

***Abstract*—Microparticles have the potentials to be used for many medical purposes in-side the human body such as drug delivery and other operations. This paper attempts to provide a thorough comparison between eight meta-heuristic search algorithms: Sparrow Search Algorithm (SSA), Flower Pollination Algorithm (FPA), Slime Mould Algorithm (SMA), Marine Predator Algorithm (MPA), Multi-Verse Optimizer (MVO) Grey Wolf Optimization (GWO), Sine-Cosine Algorithm (SCA), and Whale Optimization Algorithm (WOA). These approaches were used to calculate the PID controller optimal indicators with the application of different functions, including Integral Absolute Error (IAE), Integral of Time Multiplied by Square Error (ITSE), Integral Square Time multiplied square Error (ISTES), Integral Square Error (ISE), Integral of Square Time multiplied by square Error ((ISTSE), and Integral of Time multiplied by Absolute Error (ITAE). Every method of controlling was presented in a MATLAB Simulink numerical model, and LABVIEW software was used to run the experimental tests. . It is observed that the GWO technique achieves the highest values of settling error for both simulation and experimental results among other control approaches, while the SSA approach reduces the settling error by 50% compared to former experiments. The results indicate that SSA is the best method among all approaches and that ISTES is the best choice of PID for optimizing the controlling parameters.**

***Index Terms*—PID controller, whale optimization Algorithm, flower pollination algorithm, grey wolf optimization, sine-cosine algorithm, sparrow Search Algorithm, slime mould algorithm, marine predator algorithm, multi-verse optimizer, minimally invasive surgery**

I. Introduction

For minimizing the trauma of surgical patients, Minimal Invasive Surgery (MIS) is recommended because it provides clinicians the comfort to go deep in every site of the human body. Along with that, thanks to the minimal invasive surgery, patients are required to spend less time in hospitals. Hence, it is also a cost-effective option. Laparoscopy is one of such surgeries which are implemented these days [1].

The instruments used in this process are usually small, and the operation is conducted by observing the images taken through the instrumental camera. Different variances of the two surgical methods are exhibited in fig. 1.

Robots are used for reducing the invasiveness of minimal invasive surgery. They help in providing treatment to patients for whom surgeries are not recommended. Robotics is used to guide the accurate site for needle insertion in the body. Similarly, these robots are of great use in achieving the target required for the drug delivery, diagnosis, and treatment. In case of a smaller robot, the penetration depth inside the body is elevated leading to effective pathways of medical travel in the body.

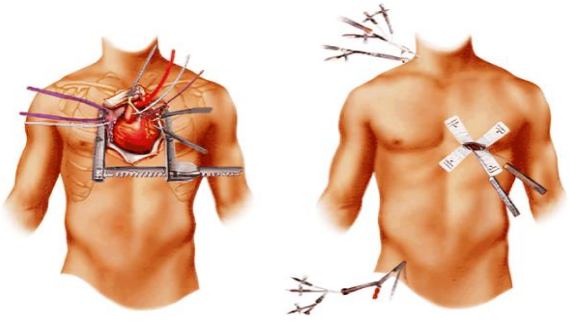

Figure 1. Image on the left exhibits an orthodox open heart surgery, whereas image on the right depicts minimal invasive surgery of heart such as laparoscopy [1].

For the spherical site, Jasper D. et al. [2] have effectively constructed paramagnetic micro particles, which have a settling error of 8.4 μm when the system arrives at the control position. The average diameter of these micro-particles was 100 μm and a hollow coil was used in the experiment. The same experiment was conducted by Ramy et al. [3] by using a solid coil, and the settling error in this experiment was 8 μm. In the present study, the same experiment was conducted and the settling error achieved was 4 μm. It was observed that the SSA approach reduced the error rate up to 50% when compared with the previous experiments.

In order to achieve control goals, a sufficient and suitable design of the controller is necessary. Although different control methods have been developed, PID is still used because of being tunable, easily implemented, and quite simple in structure [4]-[10]. However, properly tuning the PID controller in such a way to become

Manuscript received March 7, 2022; revised August 15, 2022.

doi: 10.18178/ijmerr.11.9.653-661

optimally efficient is still not easy. Among the different designs suggested, one of the best known methods of PID control is Ziegler and Nichols. However, achieving the greatest performance by this method can be challenging. Moreover, according to the usual method, tuning requires extra complex mathematical calculations [11], [12]. To avoid such different tuning, methods and artificial intelligence-based methods of optimization are preferred.

In different fields of engineering, multiple optimization techniques are used for supporting the meta-heuristic algorithms. These techniques do not require any kind of gradient information or flexibility, and their implementation is also comparatively easy. Meta-heuristic techniques include either single-based or population-based algorithms. Single-based algorithm or trajectory algorithm is the optimization algorithm in which a single optimal solution is generated, whereas other algorithms, i.e., population-based, is capable of generating multiple solutions often redundant in nature. Five major types of algorithms can be named: Human, chemical, swarm intelligence, physics, and evolutionary-based optimization algorithm [13]-[18].

The current study presents our contribution which addresses two main parts:

(i) A comparative study of six different functions: ISTSE, ITSE, ISE, ISTES, ITAE, and IAE during processing to achieve the parameters of control. The better performance of the above functions will be used to compare the dynamic characteristics of different control techniques.

(ii) A comparative study of eight novel optimization techniques; FPA, SSA, SMA, MPA, MVO, GWO, SCA, and WOA are conducted. The former techniques have been discussed for having good outcomes required to tune a controller of PID according to their settling, rising time and settling error. The tuning of PID controller is performed by minimizing the role obtained by fitness integral time square multiplied by error square.

The current study also includes mathematical model of micro-robotics system, PID controller, fitness function types, optimization techniques, and the description system architecture in part II. In part III, the simulation, experimental results, and discussion are depicted, while part IV exhibits the future prospects and conclusion of this study. The data is collected by an experimental setup, of which some results are reported in [3] which is an extension of this works.

II. Research Method

A. Mathematical Model

For designing particles, the paramagnetic material is used, and it is formed by iron-oxide in lactic acid. The diameter of these particles is 100μm, and their velocity depends on two factors. The magnetic forces and viscous drag are induced by micro-particle which depends upon the magnetic field of coils. Moreover, maximum velocity is achieved if acceleration reaches zero and magnetic and viscous drag forces are equal. The following equation is used to define the magnetic force.

$$F = \nabla \alpha_p V_p B^2 \tag{1}$$

In this equation, the volume of particles is denoted by V_p, and the magnetic flux density is denoted by B. the magnetic flux density is dependent upon the time and distance, whereas V_p and α_p are the constants. $V_p$is further substituted by using the variables given below for force production, as represented in the equation given below

$$F = \frac{4}{3}\pi \alpha_p r_p^3 \nabla B^2 \tag{2}$$

In the above-mentioned equation, the radius of micro-particles is denoted by r_p, whereas the following equation is used for drag force:

$$F_d = -6\pi\eta r_p v \tag{3}$$

Here, η represents viscosity, micro-particle's velocity is denoted by v with dependence upon the second law of motion provided by Newton.

$$\sum F = m_p a_p$$

$$\frac{4}{3}\pi \alpha_p r_p^3 \nabla^2 - 6\pi\eta r_p v = m_p a_p \tag{4}$$

$$v = \frac{\frac{4}{3}\pi \alpha_p r_p^3 \nabla B^2 - m_p a_p}{6\pi\eta r_p}$$

In equation 4, micro-particles achieve a maximum velocity when particles' acceleration equals zero. By using the following equation, the maximum velocity is calculated as follows:

$$v_m = \frac{2}{9}\frac{\alpha_p r_p^2}{\eta}\nabla B^2 \tag{5}$$

The particles with spherical shape were considered perfect, and F_m was used to denote the stimulated utilizing force. The particle's speed with respect to liquid was associated with the drag force represented byF_d. If the liquid is found stable, particle's speed is associated with the drag. The following equation is used to designate a continuous time-model.

$$m\ddot{x} + C_d * \dot{x} = F_m \tag{6}$$

As observed by C_d, there is a continuous designation of drag *via the* drag Stokes of Reynolds which is low, $\ddot{x}$ represents acceleration, $\dot{x}$ represents velocity, and the particle mass is denoted by m. The transfer role of micro-particle is signified by using the following formula:

$$\frac{X(s)}{F_m(s)} = \frac{1}{ms^2 + C_d * s} \tag{7}$$

B. PID Controller

Among the major controller types, Ideal-PID is commonly used in the industry. The algorithm of PID controller is the most vastly used in this scope. It has the ability to improve the steady state and transient errors. When disturbances occur, the ideal PID loses its high performance. Feedback control loops normally use this

algorithm as is or with minor variations [19]. These gains are proportional gain K_p, integral gain K_i, and derivative gainK_d. Every gain can act on the error which is usually achieved by subtracting a measured variable, i.e., the output from a set point that the user had inserted. Equation number 8 exhibits the PID controller's transfer function. The standard form of PID controller is illustrated in Fig. 2.

$$C_{PID}(s) = \frac{Y(s)}{E(s)} = K_p + \frac{K_i}{s} + K_d s \tag{8}$$

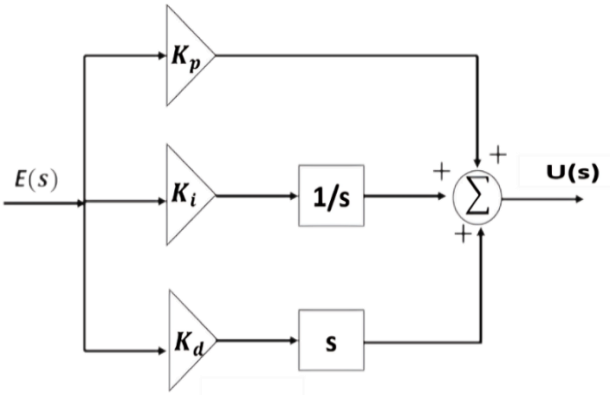

Figure 2. Block diagram of the chief ideal PID controller.

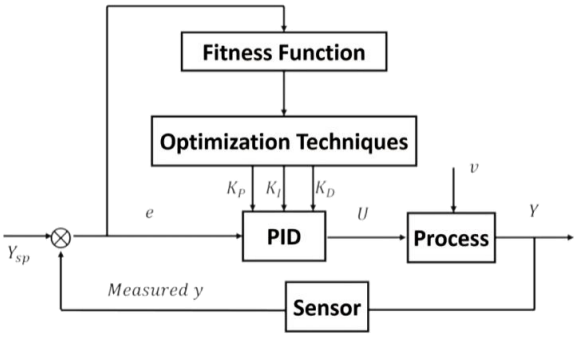

Figure 3. Block diagram of PID controller

The basic structure of PID controller is depicted in Fig. 3. The main components of PID controller are optimization techniques, process, fitness function, and sensors.

C. Fitness Functions Types

For designing any type of controllers, there are different optimum control parameters. Different parameters are computed to reduce the objective function. Due to the error of time-dependence, multiple functional objectives exist. The following equations define the different types of fitness functions [20]-[22]:

Integral Absolute Error (IAE):

$$IAE = \int_0^\infty |e(t)|dt \tag{9}$$

Integral Square Error (ISE):

$$ISE = \int_0^\infty e^2(t)\,dt \tag{10}$$

Integral of Time multiplied Absolute Error (ITAE):

$$ITAE = \int_0^\infty t|e(t)|dt \tag{11}$$

Integral of Time multiplied square Error (ITSE):

$$ITSE = \int_0^\infty te^2(t)dt \tag{12}$$

Integral Square Time multiplied square Error (ISTES):

$$ISTES = \int_0^\infty [t^2 e(t)]^2 dt \tag{13}$$

Integral of Square Time multiplied by square Error (ISTSE):

$$ISTSE = \int_0^\infty t^2 e^2(t)dt \tag{14}$$

The problem of optimization is formulated by using the following rules, i.e., objective function is minimized and subjected to:

$$K_{pmin} < K_p < K_{pmax}$$
$$K_{imin} < K_i < K_{imax}$$
$$K_{dmin} < K_d < K_{dmax}$$

D. Sparrow Search Algorithm (SSA)

As described, SSA is a technique of swarm intelligence optimization. The main idea behind this algorithm was inspired by closely observing the sparrow population behavior and the concept of foraging [23]. Depending on their behavioral characteristics, sparrows are classified into two groups: Producers and scroungers. Producers are the ones who have a larger space to locate the sources of food, and the other group which searches for food is called scroungers. The formula of SSA is determined by using the following equations.The matrix given below is used to determine the position of sparrows.

$$X = \begin{bmatrix} X_{1,1} & \cdots & X_{1,d} \\ \vdots & \ddots & \vdots \\ X_{n,1} & \cdots & X_{n,d} \end{bmatrix} \tag{15}$$

In the equation presented above, *d* represents the total dimension numbers, and *n* is the total sparrow number. In case of high energy levels in sparrows, these are called producers. They are designated to find certain areas which have rich food supply and to scavenge such zones to scroungers. Sparrow's value of cost is evaluated by the formula given below.

$$F_x = \begin{bmatrix} f(X_{1,1} & \cdots & X_{1,d}) \\ \vdots & \ddots & \vdots \\ f(X_{n,1} & \cdots & X_{n,d}) \end{bmatrix} \tag{16}$$

Once sparrows locate the producers, alarming signals are produced for other sparrows depending upon the threshold criteria. Producers lead scroungers to a safe destination if the alarm value exceeds the safety threshold value. Producers which have the best cost value are more likely to find food than the scroungers. The following equation is used to update the position of producers continuously:

$$X_{i,j}^{t+1} = \begin{cases} X_{i,j}^t * \exp\left(-\frac{i}{\beta * iter_{max}}\right) & if\ R_2 < ST \\ X_{i,j}^t + Q * L & if\ R_2 \geq ST \end{cases} \tag{17}$$

In this equation, the producer's current position in *jth* dimension present in *ith* iteration is described by $X_{i,j}^{t}$, whereas the maximum number of iterations is denoted by $iter_{max}$. The threshold value is denoted by *ST* and falls in the range of [0.5, 1], β denotes a random constant value ranging from [0 1], and the value of R_2 lies within [0, 1]. Hence, according to this equation, if the value of R_2 is lesser than the value of *ST*, there are zero predators, and producers can search for food sources globally. In other cases, R_2 is equal to or greater than *ST*. The equation used to update the position of scroungers is given below:

$$X_{i,j}^{t+1}\begin{cases} Q * \exp\left(\dfrac{X_{worest}^{t} - X_{p}^{t+1}}{i^2}\right) & if\ i > n/2 \\ X_{p}^{t+1} + \left|X_{i,j}^{t} - X_{p}^{t+1}\right| x\ \ A^{+}\ x\ L\ \ Otherwise \end{cases}$$

In this equation, A^{+} is determined by$A^{+} = A^{T} * (A * A^{T})^{-1}$, X_p is the position value found by producer, and the value of the global worst population is represented by X_{worst}. These positions are determined according to the following equation:

$$X_{i,j}^{t+1} = \begin{cases} X_{best}^{t} + \alpha * \left|X_{i,j}^{t} - X_{best}^{t+1}\right| x\ \ if\ f_i > f_g \\ X_{i,j}^{t} + K * \left(\dfrac{\left|X_{i,j}^{t} - X_{worst}^{t+1}\right|}{(f_i - f_\omega) + \varepsilon}\right)\ f_i = f_g \end{cases} \quad (19)$$

In this equation, X_{best}^{t} is the value of the current global optimal location, *K* is a random value, α is another random value which is normally distributed with a variance of 1 and a mean value of 0, f_ω is the worst fitness value, and f_i, and f_g are the current individual and global best costs respectively. The flowchart is present in Fig. 4.

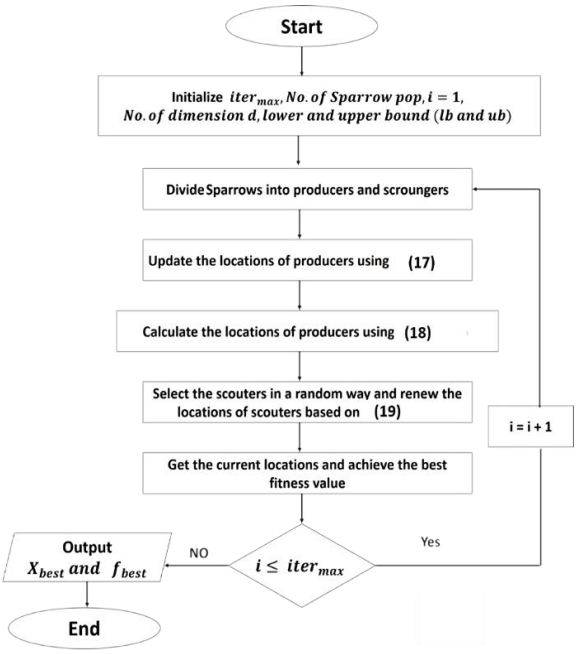

Figure 4. Flowchart of the SSA [23]

III. System Architecture

There are seven components of system architecture: Coils, control algorithms, reservoir, real time controllers, power supply units, microscope cameras, and pantograph robots. Fig. 5 displays the major components of micro-particle in 2D space. The former components are discussed in details in the following sections.

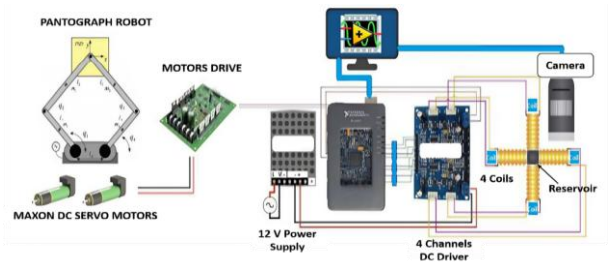

Figure 5. Micro-particle's complete system architecture in 2D space [3]

A. Real Time Controller

We used the My Rio controller to create a real-time controller and for real-time operation. As indicated in Fig.6, time control and monitoring are divided into several duties.

Figure 6. The adaptive suggested system for micro-particle controlling the in a 2D space [3].

B. Robot of Pantograph

Such a robot of pantograph contains four links with two encoders for computing the 2 chief angles. The pantograph chief role is to permit the operator to controlling the trajectory of the micro-particle. Four Angles are the pantograph chief parts. Of such angles 2 are designated as angles being passive. Such 2 angles are figured by other angles as illustrated in Fig.7. The angles that calculated are shown utilizing the formula as follows:

$$f = \begin{pmatrix} f_1 \\ f_2 \end{pmatrix} = \begin{pmatrix} l_1 cosq_1 + l_2 cosq_2 - l_3 cosq_3 - l_4 cosq_4 - l_0 \\ l_1 cosq_1 + l_2 cosq_2 - l_3 cosq_3 - l_4 cosq_4 \end{pmatrix} \quad (20)$$

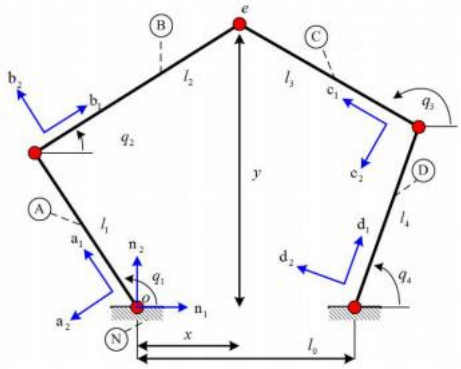

Figure 7. Pantograph kinematic [3].

C. Reservoir

It is prepared by acrylic with 10 x 10 x 9 mm dimensions as illustrated in Fig. 8.

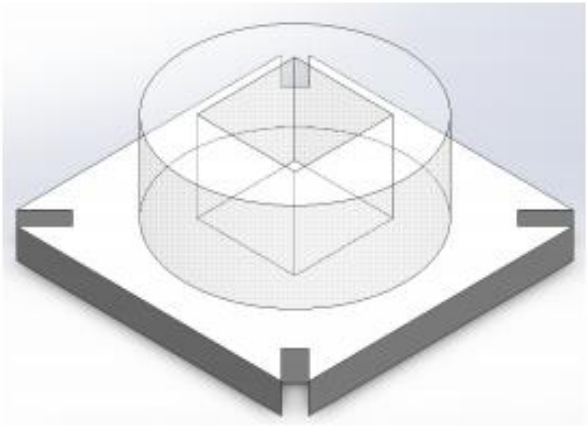

Figure 8. Reservoir [3].

D. Coils

We utilize four coils for controlling the 2D micro-particle position in the water. A COMSOL software was used for simulating the density of magnetic flux based on X and Y positions for particles coordination. The coil is made of isolated copper wire with a 0.7mm dimension diam., the turns number is 1200 as illustrated in Fig.9 and 10.

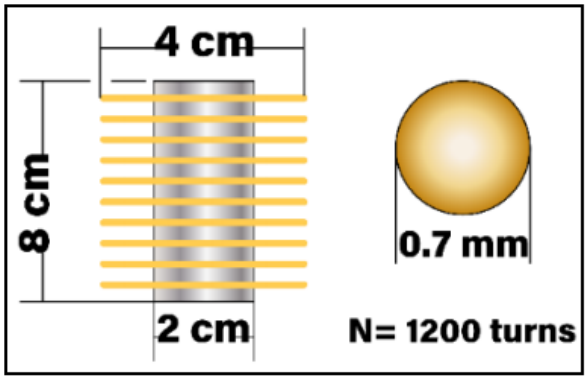

Figure 9. Dimensions of electromagnetic [3].

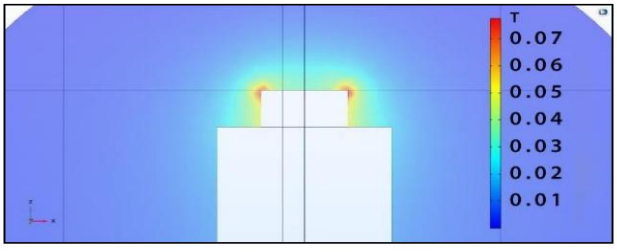

Figure 10. The density of electromagnet flux [3].

E. Devices as Peripheral

Also, we required four DC driver channels for the voltage allocation usage on the four coils. Besides, the voltage supply power is designated as 12V.

F. Setup of Camera

For avoiding camera orientation drifting from one trial to other, a simple sleeve and base were constructed for such goal. Extra over, the camera is sleeve fitted to slide on the base rail for placing the camera on the tank which is glued to the base.

G. Control Algorithm

The control algorithm application was created utilizing LABVIEW software.

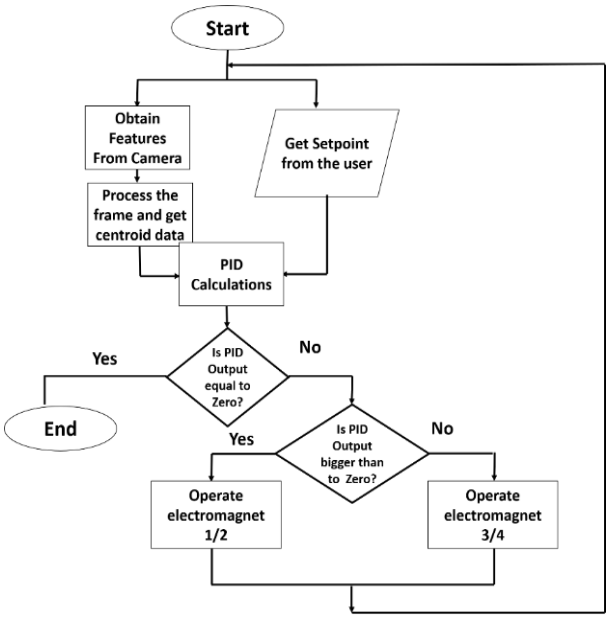

Figure 11. Control algorithm flowchart [3].

Such step gives the different merit characters that thread as multi and the high computer clock speed. The applied algorithm has 2 chief layers, the 1st one in which the data processing is done and the control signals calculation, whereas the 2nd one is the utilizer as the graphical interface (GUI). The 1st one is splitting a few tasks as sequential. Fig.11, presents a control algorithm flowchart.

IV. Results and Discussions

A. Simulation and Experimental Results

Details on investigating the performance of micro-robotics system with the use of various advanced methods of control is presented in this section. For executing and assessing the performance of various control techniques, different tests are used. For standardization, different approaches are evaluated at a particular position, i.e., for command reference, 1000 µm is used. In fig.12, the Simulink diagram is presented, and it exhibits different techniques of the micro robotic system. The proposed system parameters are presented in Table I, and a summary of various techniques parameters is given in Table II for the maintenance control of the micro-robotics system position at 1000 µm. Table III provides the output results of the various optimization techniques in terms of time response with different objective functions, while Table IV describes the output result of various optimization techniques in terms of time response (Practical) based on

the best fitness function (ISTES). Fig. 14, represents the behavior by tracking the position reference with different fitness functions, while Fig. 14, and represents the behavior by tracking the position reference with best fitness function. It is discovered that all practical values are higher than the simulation values for all optimization methods

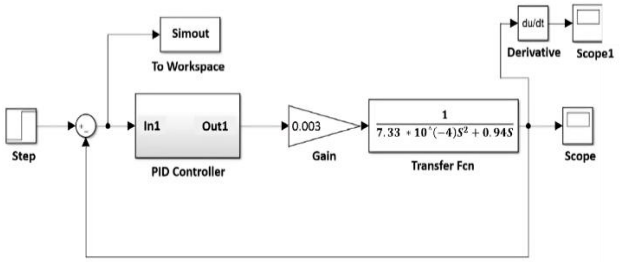

Figure 12. Simulink diagram of the micro-robotic system with different advanced control techniques.

TABLE I. THE PROPOSED SYSTEM PARAMETERS

Name	Values	Units
Radius (r)	50	μm
Density of Water (ρ)	998.2	kgm^{-3}
Dynamic Viscosity (ζ)	1	mPa s
Mass (m)	7.33*10^(-10)	Kg
Drag Coefficient (cd)	0.94*10^(-6)	N S m^{-1}

TABLE II. OPTIMIZATION TECHNIQUES INPUT PARAMETERS

Optimization Techniques	Parameters	Values
All	Number of variables (nVar)	3
	Minimum value of variables (Kmin)	[0 0 0]
	Maximum value of variables (Kmax)	[100 1 1]
	Max number of iterations	25
	Number of Search Agents	30
FPA-SMA-MPA	Probability Switch	0.8
SCA	*Parameter of SCA (a)*	*2*

TABLE III. THE OUTPUT RESULT OF VARIOUS OPIMIZATION TECHNIQUES IN TERMS TIME RESPONSE WITH DIFFERENT FITNESS FUNCTIONS (SIMULATION)

Techniques	(Ideal-PID)	Control parameter			Time response	
		KP	KI	KD	tr	ts
FPA	IAE	100	0.55445	0	6.9262	12.0955
	ISE	100	1	0	6.9574	12.0471
	ISTES	100	0.2711	0	6.9574	12.0471
	ISTSE	100	0.6051	0	6.9312	12.0948
	ITAE	100	0.2666	0	6.8895	12.0743
	ITSE	100	1	0	6.9574	12.0471
SMA	IAE	100	0.667	0	6.9368	12.0921
	ISE	100	1	0	6.9574	12.0471
	ISTES	100	0.2672	0	6.8895	12.0744
	ISTSE	100	0.6023	0	6.9309	12.0948
	ITAE	100	0.2925	0	6.8933	12.0781
	ITSE	100	1	0	6.9574	12.0471
SSA	IAE	100	0.6669	0	6.9368	12.0921
	ISE	100	1	0	6.9574	12.0471
	ISTES	100	0.2671	0	6.8895	12.0744
	ISTSE	100	0.6048	0	6.9312	12.0948
	ITAE	100	0.2956	0	6.8938	12.0785
	ITSE	100	1	0	6.9574	12.0471
MPA	IAE	100	0.667	0	6.9368	12.0921
	ISE	100	1	0	6.9574	12.0471
	ISTES	100	0.2672	0	6.8895	12.0744
	ISTSE	100	0.6048	0	6.9312	12.0948
	ITAE	100	0.2926	0	6.8934	12.0781
	ITSE	100	1	0	6.9574	12.0471
MVO	IAE	100	0.6672	0	6.9369	12.0921
	ISE	100	1	0	6.9574	12.0471
	ISTES	100	0.2667	0	6.8895	12.0743
	ISTSE	100	0.6048	0	6.9312	12.0948
	ITAE	100	0.2918	0.0034	6.8933	12.0781
	ITSE	100	1	0	6.9574	12.0471
SCA	IAE	100	0.6677	0	6.9369	12.0921
	ISE	100	1	0	6.9574	12.0471
	ISTES	100	0.2713	0.0014	6.8934	12.0782
	ISTSE	100	0.6060	0	6.9574	12.0471
	ITAE	100	0.293	0	6.9313	12.0947
	ITSE	100	1	0	6.8902	12.0751
GWO	IAE	100	0.6672	0.0891	6.9391	12.0955
	ISE	100	1	0	6.9574	12.0471
	ISTES	100	1	0	6.9574	12.0471
	ISTSE	100	0.6021	0.0019	6.9310	12.0949
	ITAE	100	0.2929	0	6.8934	12.0781
	ITSE	100	0.2926	0.018	6.8938	12.0788

WOA	IAE	100	0.666	0.0523	6.9381	12.0941
	ISE	100	1	1	6.9858	12.0875
	ISTES	100	0.2622	0.7345	6.9031	12.1035
	ISTSE	100	0.6016	0.1280	6.9341	12.0997
	ITAE	100	0.2926	0	6.8933	12.0781
	ITSE	100	1	0	6.9574	12.0471

TABLE IV. TIME RESPOSES COMPARISON AMONG VARIOUS OPTIMIZATION APPROXCHES (PARACTICAL) BASED ON BEST FITNESS FUNCTION (ISTES).

No.	Control Technique	t_r	t_s	Settling error (μm)	Reduced Based on ref[3]
1	FPA	6.9950	12.8658	5.2	35%
2	SSA	7.0294	12.1655	4	50%
3	SMA	6.9944	12.8654	5.1	36.25%
4	MVO	6.9944	12.8654	5.1	36.25%
5	MPA	6.9955	12.8670	5.3	33.25%
6	GWO	7.7083	13.1007	8	0%
7	SCA	7.0297	12.0657	5	37.5%
8	WOA	7.0505	12.0998	4.2	47.5%

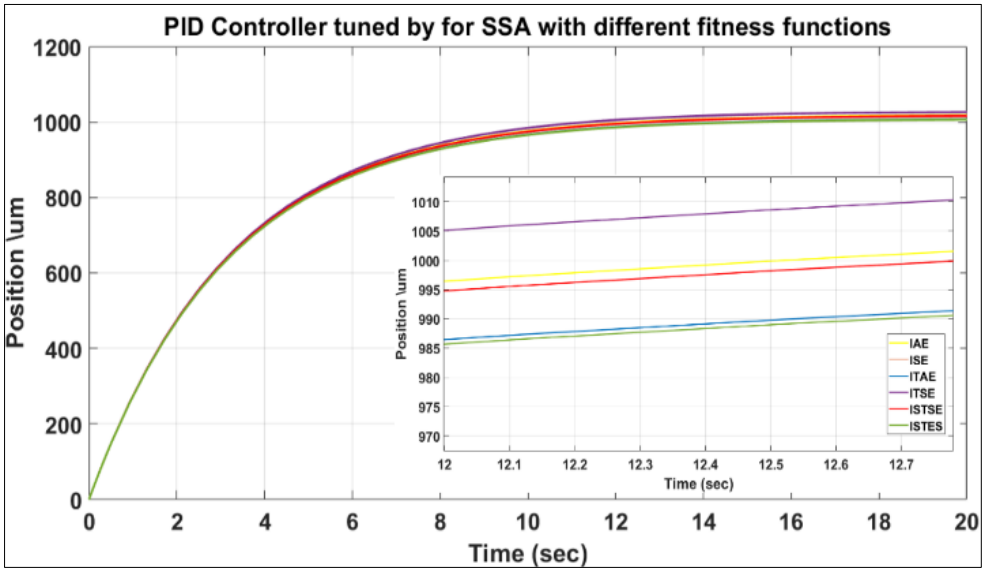

Figure 13. Position behaviour of SSA based on PID control with different fitness functions

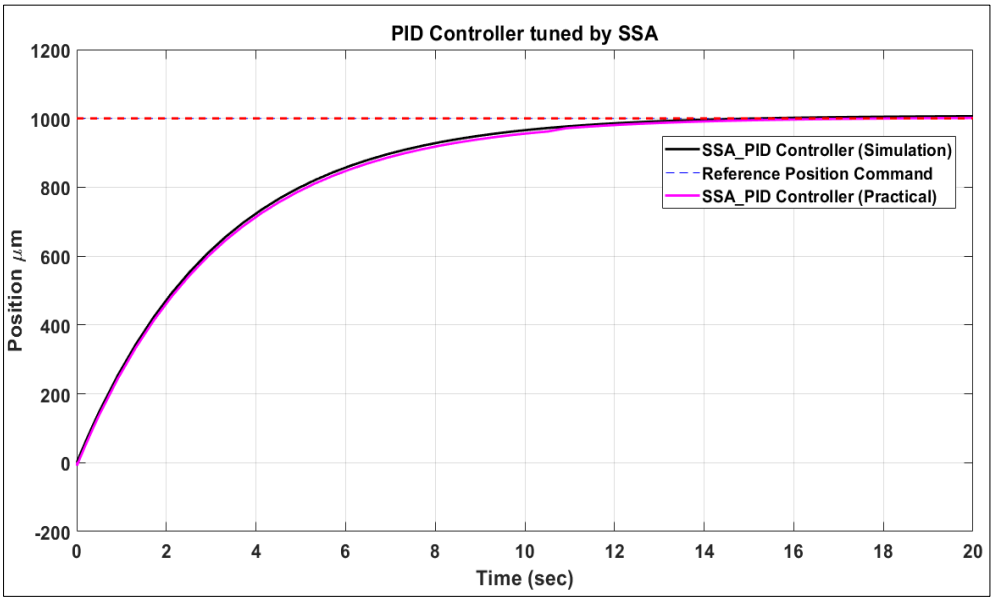

Figure 14. Position behavior with SSA based PID control

B. Discussion

In this section, the eight optimization techniques are thoroughly compared depending upon different fitness functions. The parameters consist of settling error and rising and settling time based on the best fitness function (ISTES). Table IV exhibits the results of the measurements of FPA, SMA, MVO, MPA, SSA, GWO, SCA, and WOA which have been recorded earlier. The findings show that the settling error is reduced by 33.25%, 35%, 36.25%, 36.25%, 50%, 0%, 37, 5%, and 47.5% by using MPA, FPA, SMA, MVO, SSA, GWO, SCA, and WOA respectively, compared with former experiments [3], that exhibits the highest amount of settling error It was observed that the GWO technique achieves the highest values of the rise time, settling time and settling error for both simulation and experimental results among other control approaches, while the SSA approach reduces the settling error by 50% compared to former experiments [3]. It can be concluded that the SSA technique is a promising approach for predicting real-time for the micro-robotics system.

V. Conclusions

The paper consists of eight different techniques of optimization of PID controller tuning. Based on a set of different fitness functions to discover the best performance, the ISTES achieves the highest performance. Techniques were compared on the basis of different algorithms including SSA, FPA, SMA, MPA, MVO, GWO, SCA, and WOA. It is observed that among all eight, SSA outperforms all other techniques when their rising time, setting time, and settling error are compared, and thus SSA is recommended for the tuning of PID parameters based on the best fitness function (ISTES). It is observed that SSA enhances the parameter efficiency of systems by decreasing the error rate up to 50% when compared to former experiments. For future aspects, flower pollination algorithm (FPA), sine cosine algorithm (SCA), hybrid PSO, and whale optimization algorithm (WOA) will require further investigations.

Conflict of Interest

The authors declare that there is no conflict of interests.

Author Contributions

F.A.T.: Supervision, Conceptualization and Reviewing and Editing. E.S.G.: Methodology, Software, validation, Writing-Original draft preparation, Formal analysis. All authors have read and approved to the final manuscript.

Acknowledgment

I would like to thanks Dr. Mohamed Sallam for his support in the experimental setup.

References

[1] J. Keuning. “Image-based magnetic control of microparticles,” Master's thesis, University of Twente, 2011.

[2] J. D. Keuning, J. de Vriesy, L. Abelmanny, and S. Misra, "Image-based magnetic control of paramagnetic microparticles in water", in *Proc. 2011 IEEE/RSJ International Conference on Intelligent Robots and Systems*, 2011, September, pp. 421-426.

[3] R. Farag, I. Badawy, F. Magdy, Z. Mahmoud, and M. Sallam, "Real-time trajectory control of potential drug carrier using pantograph “Experimental Study,” in *Proc. International Conference on Advanced Intelligent Systems and Informatics*, 2020, October, pp. 305-313, Springer, Cham.

[4] J. K. Astrom and T. Hagglund, “PID Controllers: Theory, design, and tuning,” 2nd ed.: NC: Instrument Society of America, 1995.

[5] M. Tamer, “PID controller implementation and tuning,” Published by InTech.2011.

[6] K. Ogata, *Modern Control Engineering*, *Prentice-Hall*, 2010.

[7] T. Hägglund and K. J. Åström, “Revisiting the Ziegler-nichols tuning rules for PI control,” *Asian J. Control*, vol. 4, no. 4, pp. 364-380,2002.

[8] W. Tan, J. Liu, T. Chen, and H. J. Marquez, “Comparison of some well-known PID tuning formulas,” *Comput. Chem. Eng.*, vol. 39, no. 9, pp. 1416-1423, 2006.

[9] A. Visioli, “Research trends for PID controllers,” *Acta Polytech.*, vol. 52, no. 5, 2012.

[10] D. Valério and J. S. Da Costa, “Tuning of fractional PID controllers with Ziegler–Nichols-type rules,” *Signal Process*, vol. 86, no. 10, pp. 2771-2784, 2006.

[11] D. K. Maghade and B. M. Patre, “Pole placement by PID controllers to achieve time domain specifications for TITO systems,” *Trans. Inst. Meas. Control*, vol. 36, no. 4, pp. 506-522, 2014.

[12] Z. Bingul and O. Karahan, "Comparison of PID and FOPID controllers tuned by PSO and ABC algorithms for unstable and integrating systems with time delay," *Optim Control Appl Methods*, vol. 39, no. 4, 1431-1450, 2018.

[13] E. S. Ghith, F. A Tolba, and S. A. Hammad, "Real-time implementation of tuning PID controller based on sine cosine algorithm for micro-robotics system," in *Proc. International Conference on Digital Technologies and Applications*, 2022, pp. 801-811.

[14] E. S.Ghith and F. A. A. Tolba, "Real-time implementation of tuning PID controller based on whale optimization algorithm for micro-robotics system," in *Proc. 2022 14th International Conference on Computer and Automation Engineering (ICCAE)*, 2022, pp.103-109.

[15] D. Yousri, M. A. Elaziz, and S. Mirjalili, “Fractional-order calculus-based flower pollination algorithm with local search for global optimization and image segmentation,” *Knowl Based Syst*, vol. 197, pp. 105889, 2020.

[16] E. S. Ghith and F. A. A. Tolba, "Design and optimization of PID controller using various algorithms for micro-robotics system,” *Journal of Robotics and Control (JRC)*, vol. 3, no. 3, pp. 244-256, 2022.

[17] S. Li, H. Chen, M. Wang, A. A. Heidari, and S. Mirjalili, “Slime mould algorithm: A new method for stochastic optimization,” *Future Generation Computer Systems*, vol. 111, pp. 300-323, 2020.

[18] A. Yakout, W. Sabry, and H. M. Hasanien, “Enhancing rotor angle stability of power systems using marine predator algorithm-based cascaded PID control,” *Ain Shams Eng. J.*, vol. 12, no. 2, pp. 1849-1857, 2021.

[19] K. J. Astrom and T. Hagglund, *PID Controllers: Theory, Design, and Tuning*, 2nd ed., NC: Instrument Society of America, 1995.

[20] M. M. Eissa, G. S. Virk, A. M. AbdelGhany, and E. S. Ghith, "Optimum induction motor speed control technique using genetic algorithm," *American Journal of Intelligent Systems(AJIS)*, vol. 3, April 2013, California, USA.

[21] M. M. Eissa, G. S. Virk, A. M. AbdelGhany, and E. S. Ghith, "Optimum induction motor speed control technique using particle swarm optimization,” *International Journal of Energy Engineering(IJEE)*, vol. 3, no. 2, March 2013, California, USA.

[22] M. Sallam, I. Saif, Z. Saeed, and M. Fanni. "Lyapunov-based control of a teleoperation system in presence of time delay,” in *Proc. International Conference on Advanced Intelligent Systems and Informatics*, pp. 759-768. Springer, Cham, 2020.

[23] J. Xue and B. Shen, "A novel swarm intelligence optimization approach: Sparrow search algorithm," *Syst. Sci. Control Eng*, vol. 8, no. 1, pp. 22-34, 2020.

Ehab Saif Ghith is born in Cairo, Egypt, on August 23, 1978. He received the B.Sc. degree in Design and Production Engineering in 2002 from the Faculty of Engineering at Ain shams University, Cairo, Egypt, M. Sc. in Systems Engineering and Engineering management, South Westphalia University of Applied Sciences, Germany 2013 and M.Sc. in System's Automation and Engineering Management, Helwan University, Egypt, 2013, Research topic: "Optimum induction Motor speed control technique using intelligent Methods". His research activity includes studying Artificial Intelligence, Electrical Machines, Automatic Control and Robotics.He can be contacted at email:Drehabghith1978@gmail.com

Farid Abdel Aziz Tolba is born in Cairo, Egypt, on August 1, 1944. He received the B.Sc. degree in Design and Production Engineering in 1969 from the Faculty of Engineering at Ain shams University, Cairo, Egypt, M. Sc. and PhD in Design and Production Engineering, 1972 and 1975 respectively, (Teaching Assistant on 1969-09-13--Assistant Lecturer on 1972-12-04-Lecturer on: 1975-10-27- Assistant Professor on1980-12-01-Professor on 1986-02-03- Emeritus on 2004-08-01. His research activity includes studying Artificial Intelligence, Automatic Control and Robotics. He can be contacted at email:farid_tolba@eng.asu.edu.eg